ISSN: 2710-0588

Research on the Correction of Soil Pressure Distribution Pattern in Circular Working Wells in Soft Soil Areas

Minjian Long, Zhicheng Bai*, Zhiyuan Zhang, Zhenjie Tan

China Construction Fourth Engineering Bureau Sixth Construction Co., Ltd., Shanghai 201100, China

*Corresponding Author: 463803941@qq.com

Abstract

This paper investigates the distribution characteristics of earth pressure on circular caisson foundations in soft soil areas based on practical engineering considerations. Utilizing a three-dimensional numerical analysis model and a displacement-based method for earth pressure calculation, the lateral earth pressure on the retaining structure is examined. Adjustments are made to the distribution pattern of earth pressure on circular caisson foundations in soft soil areas. The study demonstrates that the radius of the caisson significantly influences the spatial distribution of soil pressure. Additionally, empirical formulas for the depth and radius of the reduction in soil pressure around circular caisson foundations are obtained through the research. Comparative analysis reveals that the modified earth pressure planar foundation beam method, which accounts for the arching effect, is simpler, features more mature parameter selection, and is more cost-effective than the three-dimensional finite element method. In comparison to the standard planar elastic foundation beam method for earth pressure, it aligns more closely with the actual direction of displacement.

Keywords

Soft Soil Areas; Circular Working Well; Spatial Arch Effect; Distribution Pattern of Soil Pressure.

1. Introduction

Most excavation accidents are caused by inaccurate calculation of soil pressure. Circular foundation pits have two advantages: firstly, the retaining structure of the foundation pit will form a circular whole, and this closed arch structure can make the retaining structure have circumferential compression characteristics, thereby fully utilizing the high compressive strength of concrete materials [2]; Secondly, the soil outside the circular foundation pit will produce a significant "soil arching" effect, resulting in lower soil pressure acting on the circular support structure than on the straight edge foundation pit. Therefore, more and more foundation pits are designed with circular structures [3].

At present, there is limited research literature on the soil pressure of circular foundation pits, and research methods are mainly limited to the limit equilibrium method and sliding line method. The obtained results are only applicable to the ideal situation of uniform soil, horizontal ground, and smooth vertical walls. Berezanzev [4] used the sliding line method to solve the soil pressure problem of an ideal circular foundation pit. Prater [5] summarized the limit equilibrium solution of active soil pressure in circular foundation pits, introduced the circumferential stress coefficient, and analyzed its impact on soil pressure. Cheng et al. based on Prater's theory, assumed that the slip line is two sets of parallel straight lines, introduced the circumferential stress coefficient, and solved the simplified slip line solution for circular vertical axis soil pressure. Liu Faqian [7] considered the influence of various factors on soil

ISSN: 2710-0588

pressure based on slip line theory; Based on the theory of limit analysis, the upper limit solution of active soil pressure for circular foundation pits was derived. Zai Jinmin et al. proposed a new method for calculating soil pressure on retaining walls. Lu Guosheng et al. [11] considered the influence of displacement when calculating soil pressure and compared the calculation results with the finite element calculation results. Chen Yekai [12-14] described the relationship between soil pressure acting on retaining walls and wall displacement using an exponential function, and calculated the soil pressure acting on retaining walls under non limit state conditions.

The theoretical research results on the soil pressure of circular foundation pits are not yet complete. This article takes the municipal comprehensive renovation project of Shanghai Hongqiao Business District as the background and intends to study the distribution pattern of soil pressure in circular working wells in soft soil areas. Established a three-dimensional numerical analysis model for well soil. Taking into account factors such as wall insertion rate, working well radius, wall thickness, and wall elastic modulus, the influence of working well spatial arch effect on the distribution pattern of soil pressure was explored. On the basis of the current Shanghai Engineering Construction Specification "Technical Specification for Foundation Pit Engineering" [15], a soil pressure distribution model for circular working wells in soft soil areas is proposed and verified through engineering examples.

2. Project Overview

The Shanghai Hongqiao Business District Municipal Comprehensive Renovation Project is located in a soft soil area, including 2 working wells, 2 receiving wells, and 1 inlet gate well. Among them, the 4 # working well is a circular structure with a diameter of 14m and a depth of 15m, belonging to a deep and large foundation pit, which requires high safety and stability. The vertical shaft is surrounded by a double row drilled cast-in-place pile water stop curtain, with a length of 23m and a wall thickness of 1.5m, as shown in the following figure. The working well is not supported and constructed using the layered reverse construction method. The excavation of the vertical shaft is divided into three steps. The specific construction conditions are shown in Table 1. The basic soil layer parameters are shown in Table 2.

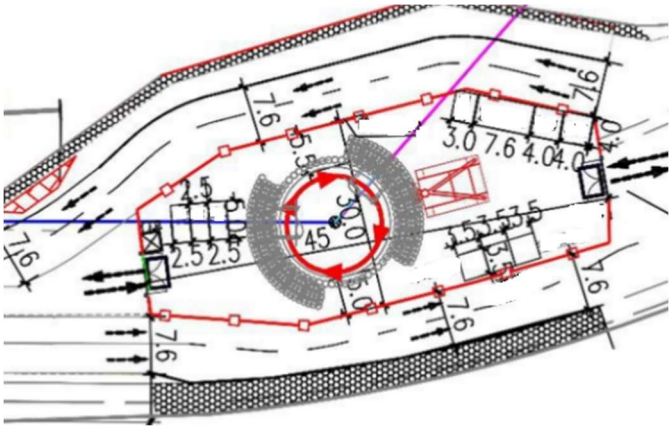

Figure 1. Schematic diagram of the plane position of work well 4 #

Table 1. Construction conditions

working condition	Excavation depth and lining pouring
Working condition one	5m, pour lining within the depth range of 0-5m
Working condition two	10m, pour lining within a depth range of 5-10m
Working condition three	15m, pour inner lining and bottom plate within a depth range of 10-15m

ISSN: 2710-0588

Table 2. Basic soil layer parameters

Numble	Soil layer	Thickness (m)	severe γ(kN/m^3)	Initial porosity ratio e_0	Cohesive force c(kPa)	Poisson's ratio v
1	Cohesive soil	2.3	18.82	0.94	15	0.47
2	Silt Silty Clay	5.6	17.85	1.18	17	0.35
3	muddy clay	6.9	17.15	1.43	16	0.4
4	Brown cohesive soil	7.3	18.25	1.03	15	0.35
5	Green cohesive soil	1.8	19.8	0.71	15	0.3
6	Fine sand	21	19.25	0.76	6.7	0.3
7	Clay mixed with silt	33	18.45	0.94	-	0.61

3. A Three-dimensional Finite Element Analysis Model for the Interaction between Well and Soil

3.1. Finite Element Analysis Model

Correcting the Cambridge model requires four calculation parameters [17], namely the slope of the normal consolidation line in the v-lnp 'plane λ, The slope k of the rebound line in the v-lnp 'plane, the slope M of the CSL on the p' - q 'plane, and the Poisson's ratio v. Among them, λ, k. M can be obtained from the following equation:

$$\lambda = \frac{C_c}{\ln 10} \tag{1}$$

$$k = \frac{C_s}{\ln 10} \tag{2}$$

$$M = \frac{6\sin\varphi'}{3-\sin\varphi'} \tag{3}$$

In the formula, CC is the compression index of the soil, and CS is the rebound index of the soil, φ' The effective internal friction angle obtained from the triaxial compression test.

This article adopts a finite sliding Coulomb friction model to simulate the friction between the retaining structure and the soil. In the Coulomb friction model, two contact surfaces generate equivalent shear stress at their interface before sliding against each other τ Equal:

$$\tau_{equal} = \sqrt{\tau_{FS1}^2 + \tau_{FS2}^2} \tag{4}$$

In the formula, τ FS1 is the shear (friction) stress in the 1 direction on the contact surface; τ FS2 is the shear (friction) stress in the 2 directions on the contact surface.

Critical shear stress τ Crit is directly proportional to the normal contact stress P, expressed as follows:

$$\tau_{crit} = \mu P \tag{5}$$

In the formula, μ Is the coefficient of friction.

ISSN: 2710-0588

Critical shear stress τ CRIT sets the ultimate shear stress, and the critical shear stress can be expressed as:

$$\tau_{crit} = \min(\mu P, \tau_{max}) \quad (6)$$

Among them, τ Crit is the ultimate shear stress, and for the problem of the interaction between underground continuous walls and soil, τ Max is equivalent to the ultimate lateral frictional resistance of an underground continuous wall.

When the equivalent shear stress on the contact surface τ Equal exceeds critical shear stress τ During CRIT, relative sliding occurs between the contact surfaces, as shown in Figure 2.

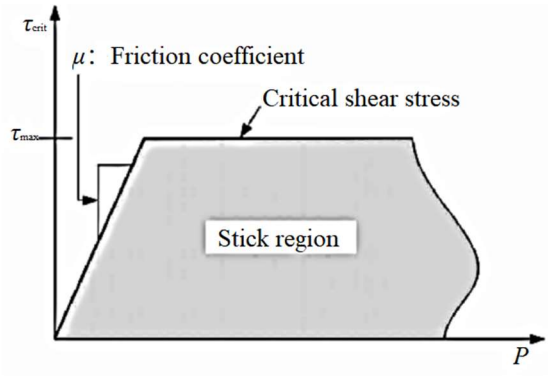

Figure 2. Coulomb friction characteristics [17]

Table 3 lists the basic calculation parameters of typical soil layers in soft soil areas, including the effective internal friction angle φ', Lateral pressure coefficient K0 and compression curve slope λ, The slope k of the rebound curve, critical state parameter M, and Young's modulus E can be obtained based on the above formula and relevant literature.

The contact surface parameters include the ultimate lateral friction resistance of the continuous wall τ Max and wall soil friction coefficient μ, among τ Max refers to the standard value of ultimate lateral friction resistance of cast-in-place piles in the "Code for Geotechnical Engineering Investigation" [18], and the wall soil friction coefficient μ Refer to the recommended values for the friction coefficient between the bottom of the pile foundation cap and the foundation soil in the National Technical Specification for Building Pile Foundations [19]. Please refer to Table 4 for details.

Table 3. Basic calculation parameters of typical soil layers in soft soil areas

Numble	Effective internal friction angle ψ'(°)	Lateral pressure coefficient K_0[20]	Compression curve slope λ[21-22]	Slope of rebound curve k[23]	Critical state parameters M	Young's modulus E(MPa)[24]
1	32	0.3	0.12	0.01	0.6	-
2	29	0.52	0.1	0.008	0.55	-
3	18	0.69	0.16	0.013	0.66	-
4	32	0.47	0.11	0.009	0.45	-
5	30	0.5	0.06	0.005	0.5	-
6	33	0.45	-	-	-	95
7	23	0.3	0.16	0.013	0.9	-

ISSN: 2710-0588

Table 4. Parameters of contact surfaces between different soil layers

Numble parameter	1	2	3	4	5	6	7
τ_{max}(kPa)	20	20	22	35	62	75	55
μ	0.3	0.25	0.25	0.35	0.3	0.4	0.35

The thickness of the underground continuous wall is 1.8m, the thickness of the inner lining is 0.8m, and the retaining structure adopts a linear elastic model. The elastic modulus of the retaining structure is taken as C30 concrete, which is 3 × 1010Pa, and the Poisson's ratio is 0.2. This article uses the finite element software Abaqus to conduct three-dimensional finite element simulation of a circular vertical shaft. Combined with the above working conditions, the simulation process is shown in the following figure:

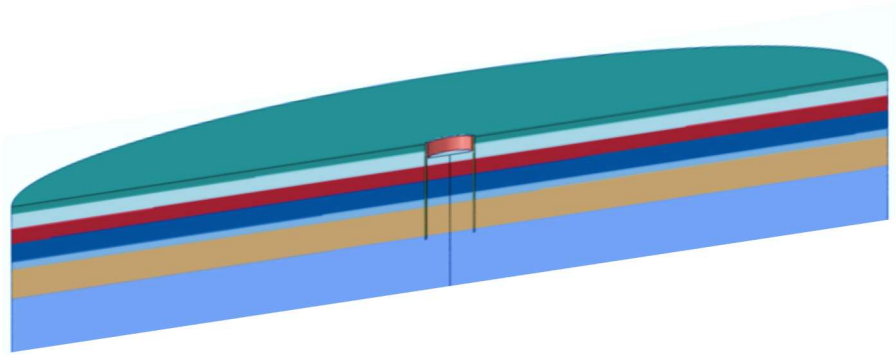

(a) Mode I model

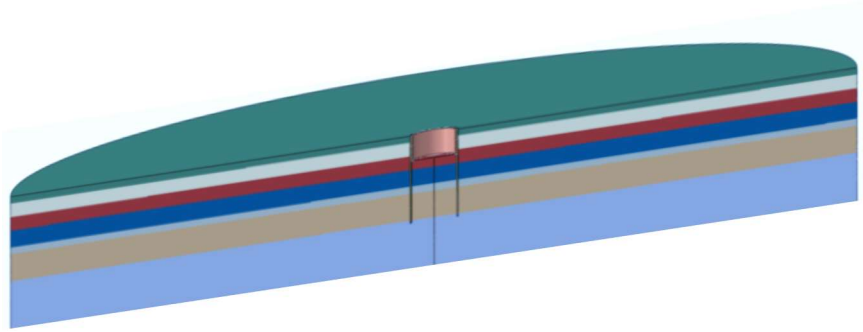

(b) Mode 2 model

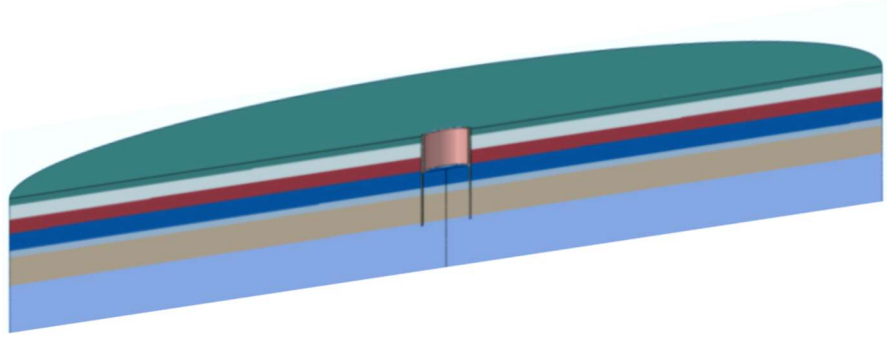

(c)Mode 3 model

Figure 3. Three dimensional finite element analysis model of circular working well

ISSN: 2710-0588

3.2. Numerical Result Analysis

The three-dimensional finite element numerical simulation results and measured values of lateral displacement of the enclosure structure are shown in Figure 4. It was found that the maximum lateral displacement of the retaining structure at each excavation depth mostly occurred near the excavation face. As the excavation depth increased, the position where the maximum lateral displacement occurred also shifted downwards. And the calculated maximum lateral displacement is consistent with the measured lateral displacement value. When reaching the maximum excavation depth, the calculated maximum lateral displacement value is 2.8mm, while the measured maximum lateral displacement value is 3.0mm. The ratio of the maximum lateral displacement of the wall to the excavation depth is about 0.02%, and the relative lateral displacement is relatively small. The lateral displacement at the top and bottom of the wall is very small.

This article refers to the distribution pattern of soil pressure in the Technical Specification for Excavation Engineering [15], and uses the plane elastic foundation beam method considering the circular arch effect to numerically simulate the actual working conditions, as shown in Figure 5. It can be seen that above the excavation surface, the lateral displacement of the retaining structure using the soil pressure distribution mode in the specifications is basically consistent with the measured displacement trend, but there is a certain difference in numerical values; But below the excavation surface, the trend of the two changes is not the same. The measured displacement value decreases with the increase of excavation depth, while the lateral displacement of the retaining structure calculated using the plane elastic foundation beam method of standard soil pressure remains basically unchanged below the excavation surface. There is a difference between the two, and the greater the depth, the more obvious this difference. This indicates that the distribution pattern of soil pressure in existing specifications cannot reflect the true deep soil pressure, and there is a certain deviation between the calculated results and the actual situation.

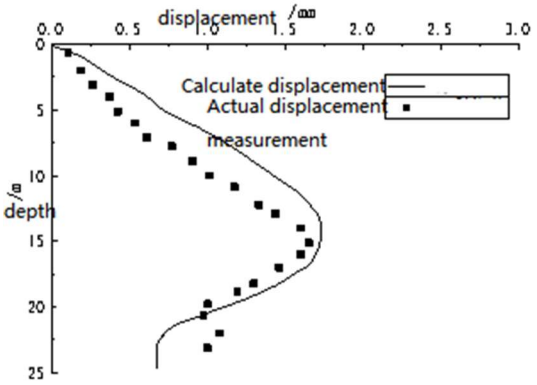

(a) Working condition one

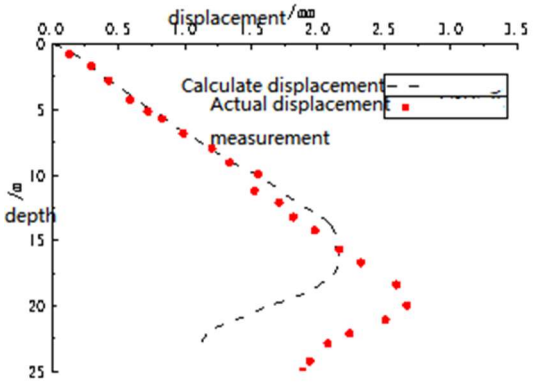

(b)Working condition two

ISSN: 2710-0588

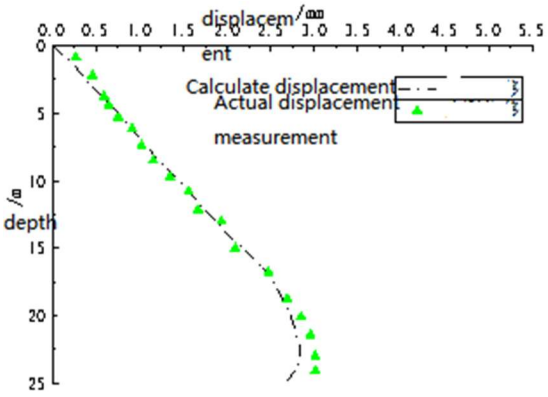

(c)Working condition three

Figure 4. Comparison between numerical results and measured values of lateral displacement of circular working well enclosure structure

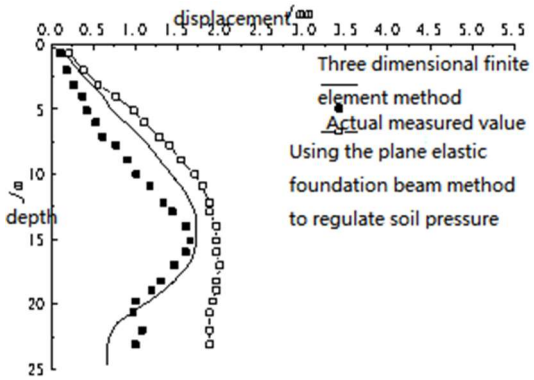

(a) Working condition one

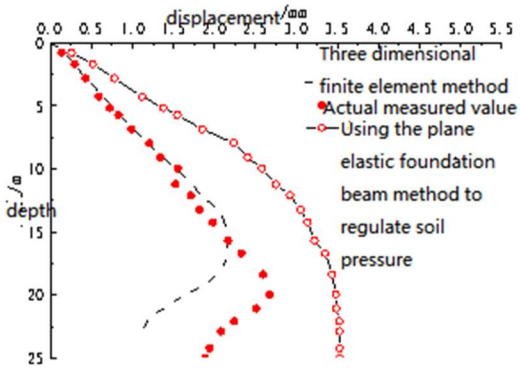

(b) Working condition two

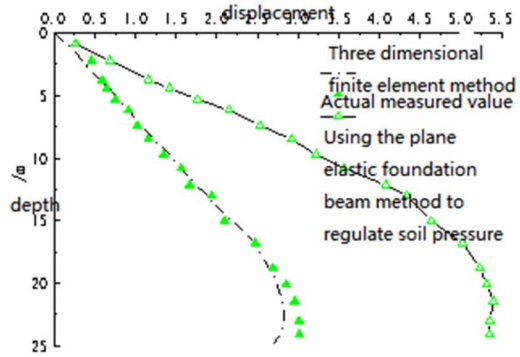

(c) Working condition three

Figure 5. Comparative analysis of lateral displacement of circular working well enclosure structure

ISSN: 2710-0588

4. Calculation Method of Soil Pressure Considering Displacement Effect

4.1. Soil Pressure Calculation Model

To fully consider the nonlinear relationship between soil pressure and displacement on the retaining structure, equations for the passive and active soil pressure relationships are established separately:

$$P_P = P_0 + (P_{Pcrit} - P_0) \left|\frac{\Xi}{\Xi_{Pcrit}}\right| e^{\xi\left|1-\frac{\Xi}{\Xi_{Pcrit}}\right|} \tag{7}$$

$$P_A = P_0 - (P_0 - P_{Acrit}) \left|\frac{\Xi}{\Xi_{Acrit}}\right| e^{\xi'\left|1-\frac{\Xi}{\Xi_{Acrit}}\right|} \tag{8}$$

In the formula, PP is the passive earth pressure; PA is the active earth pressure; P0 is the static soil pressure; PPcrit is the passive earth pressure in the ultimate equilibrium state; PAcrit is the active earth pressure in the ultimate equilibrium state; Ξ For wall displacement; Ξ Pcrit is the ultimate equilibrium state displacement when the wall is squeezed towards the soil; Ξ Acrit is the ultimate equilibrium state displacement when the wall leaves the soil; ξ, ξ' For parameters related to soil properties and other factors, $0 \le \xi \le 1$, $0 \le \xi' \le 1$.

Based on the above equation, when Ξ= At 0, PP=PA=P0; When Ξ=Ξ Pcrit, PP=PPcrit; When Ξ=Ξ Acrit, PA=PAcrit, which satisfies the boundary conditions.

For any given displacement, a tangent can be drawn through the corresponding point on the curve [14], and the soil pressure can be expressed as.

$$P_P = P_0 + \Lambda_P \cdot \xi \tag{9}$$

$$P_A = P_0 + \Lambda_A \cdot \xi \tag{10}$$

In the formula, Λ P is the coefficient of reaction of the foundation in front of the wall; Λ A is the coefficient of foundation reaction behind the wall.

Furthermore, it can be concluded that:

$$\Lambda_{\mathrm{P}} = \frac{P_{Pcrit}-P_0}{\Xi_{Pcrit}} \cdot e^{\xi\left|1-\frac{\Xi}{\Xi_{Pcrit}}\right|} \tag{11}$$

$$\Lambda_{\mathrm{A}} = \frac{P_{Acrit}-P_0}{\Xi_{Acrit}} \cdot e^{\xi'\left|1-\frac{\Xi}{\Xi_{Acrit}}\right|} \tag{12}$$

When ξ= 0 ξ'= At 0, further results are obtained:

$$\Lambda_{\mathrm{P}} = \frac{P_{Pcrit}-P_0}{\Xi_{Pcrit}} \tag{13}$$

$$\Lambda_{\mathrm{A}} = \frac{P_{Acrit}-P_0}{\Xi_{Acrit}} \tag{14}$$

ISSN: 2710-0588

4.2. Model Rationality Analysis

By comparing the soil pressure calculated by equations (4.1) and (4.2) with the three-dimensional finite element analysis model, it was found that the values and trends of the two were relatively consistent, effectively verifying the feasibility of calculating soil pressure using the three-dimensional finite element analysis model and providing a reliable basis for subsequent research.

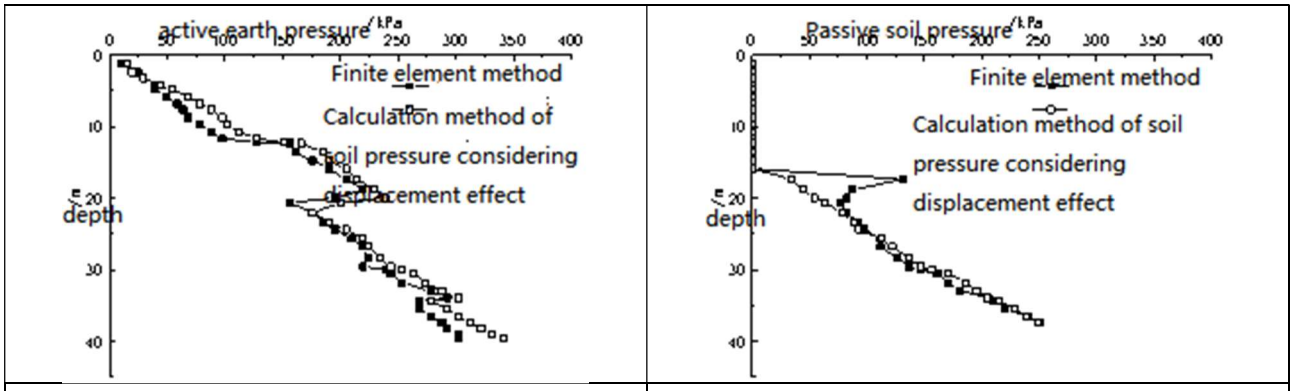

(a)active earth pressure (b)Passive soil pressure

Figure 6. Distribution of soil pressure during excavation of a circular working well (15m)

The results of soil pressure under each working condition are shown in Figure 7. It is found that the distribution of soil pressure below the excavation surface does not follow the constant distribution pattern of existing specifications, but starts to decrease from a certain depth. At a certain depth, the soil pressure can be considered zero, and the smaller the excavation depth, the more obvious this phenomenon is.

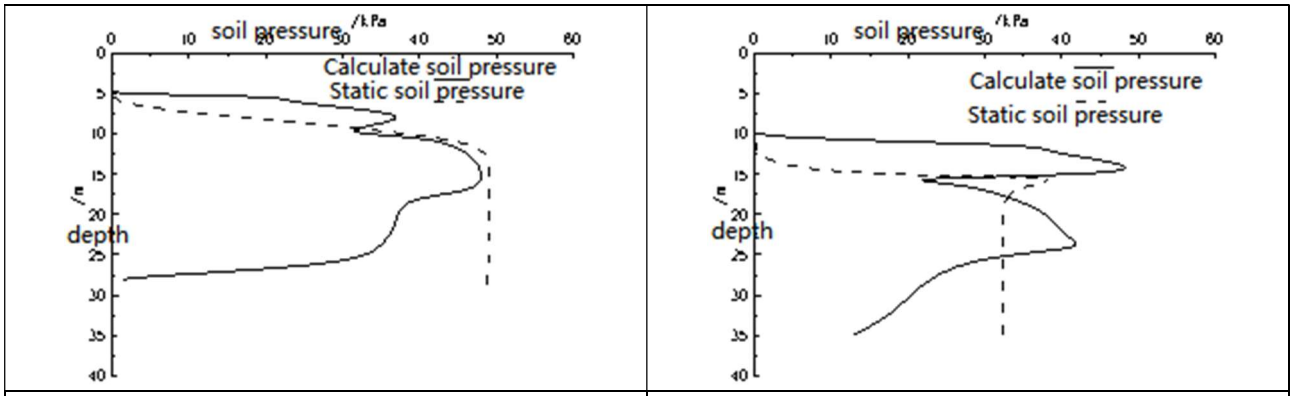

(a)Excavation to a depth of 5m with incremental soil pressure (b)Excavation to a depth of 10m with incremental soil pressure

Figure 7. Increment of soil pressure under different working conditions in circular working wells

5. The Influence of the Arch Effect of the Working Well Space on the Distribution Pattern of Soil Pressure

Based on the three-dimensional numerical analysis model of well soil, factors such as wall insertion ratio, working well radius, wall thickness, and wall stiffness are considered to explore the influence of working well spatial arch effect on the distribution pattern of soil pressure.

ISSN: 2710-0588

5.1. Influence of Wall Insertion Ratio

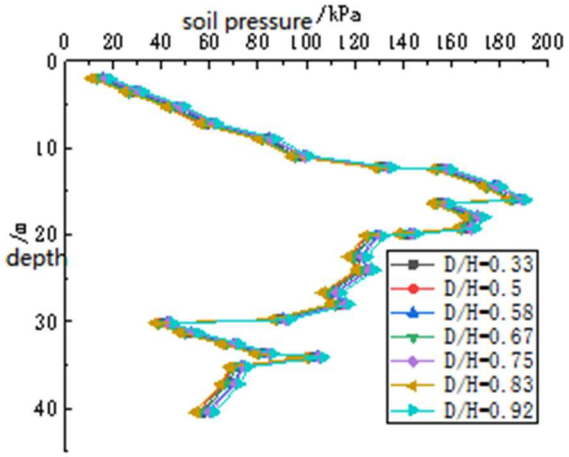

Figure 8. Lateral soil pressure of working well under different insertion ratios (excavation depth 15m)

Figure 8 shows the relationship between the lateral soil pressure of the working well and the depth under the condition of excavation depth of 15m, with wall insertion ratios of 0.33, 0.5, 0.58, 0.67, 0.75, 0.83, and 0.92, respectively. It can be observed that when the wall insertion ratio is changed, the variation trend of lateral soil pressure along the depth direction of the circular vertical shaft is basically the same. In other words, the size of the wall insertion ratio has a relatively small impact on the distribution pattern of lateral soil pressure in circular vertical shafts.

5.2. Impact of Working Well Radius

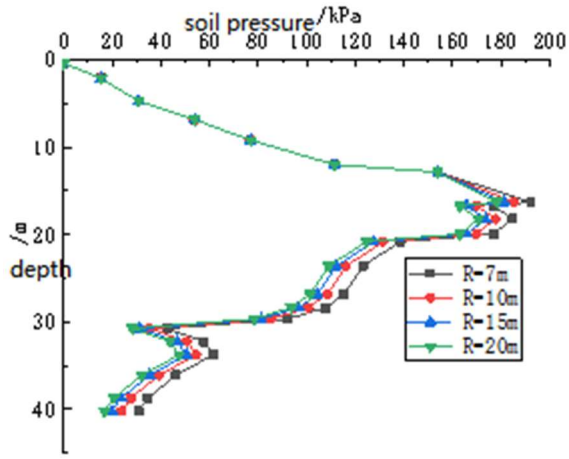

Figure 9. Lateral soil pressure of working well under different radius conditions (excavation depth of 15m)

Figure 9 shows the relationship between lateral soil pressure and depth under the condition of excavation depth of 15m, with working well radii of 7m, 10m, 15m, and 20m, respectively. As shown in the figure, when the radius of the working well is changed, the trend of lateral soil pressure changes along the depth direction is basically the same, and the values above the excavation surface are basically the same; But there is a certain difference in the values below the excavation surface, and as the radius increases, the soil pressure shows a decreasing trend. In other words, the radius of the working well has a more prominent impact on the distribution pattern of lateral soil pressure, and as the radius increases, the spatial arching effect becomes less pronounced.

ISSN: 2710-0588

5.3. Wall Thickness Influence

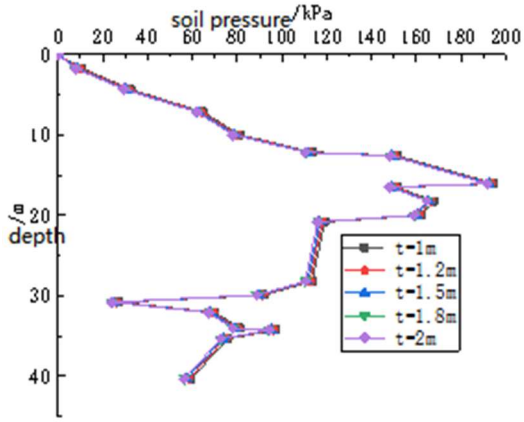

Figure 10. Lateral soil pressure of working well under different wall thicknesses (excavation depth of 15m)

Figure 10 shows the relationship between the lateral soil pressure of a circular working well and the depth when the thickness of the underground continuous wall is 1m, 1.2m, 1.5m, 1.8m, and 2m, respectively. It was found that when the thickness of the wall was changed, the trend of soil pressure in the depth direction of the circular shaft was basically the same, and the influence of the thickness change on the distribution pattern of soil pressure in the circular shaft was minimal.

5.4. The Influence of Wall Elastic Modulus

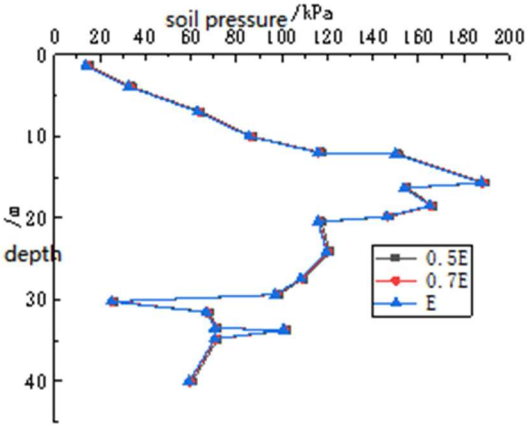

Figure 11. Lateral soil pressure of working well under different wall elastic modulus conditions (excavation depth 15m)

Figure 11 shows the relationship between the lateral soil pressure of a circular working well and depth when the elastic moduli of the underground continuous wall are 0.5E, 0.7E, and E. It was found that when the elastic modulus of the wall was changed, the soil pressure of the circular vertical shaft also showed a similar trend of change along the depth direction, and the value remained almost unchanged.

6. Correction of Soil Pressure Mode for Circular Working Wells in Soft Soil Areas

6.1. Correction of Soil Pressure Distribution Pattern

Furthermore, the radius of the working well is taken as the main research factor to study the distribution pattern of soil pressure in circular working wells in soft soil areas. Considering the

ISSN: 2710-0588

analysis conclusion in Section 3, the existing soil pressure distribution model in the specification [15] cannot reflect the true deep soil pressure. Therefore, based on this, a correction is made and a circular vertical shaft soil pressure distribution model in soft soil areas is proposed. For circular working wells in soft soil areas, the distribution of soil pressure above the excavation surface is basically consistent with the existing distribution pattern of regulations; The soil pressure below the excavation surface decreases from a certain depth (point A) to a certain depth (point B), and can be considered zero. The soil pressure in section AB is linearly reduced. The relationship between the depth of the starting point (point A) and the depth of the ending point (point B) and the excavation depth, as well as their fitting curves, for the reduction of soil pressure on working wells with different radii below the excavation surface based on static soil pressure, are shown in the following figure. The fitting formulas are obtained:

$$H_{\text{Start}} = (0.019R + 1.89) \cdot H_0 \tag{15}$$

$$H_{Fini} = (0.13R + 1.95) \cdot H_0 \tag{16}$$

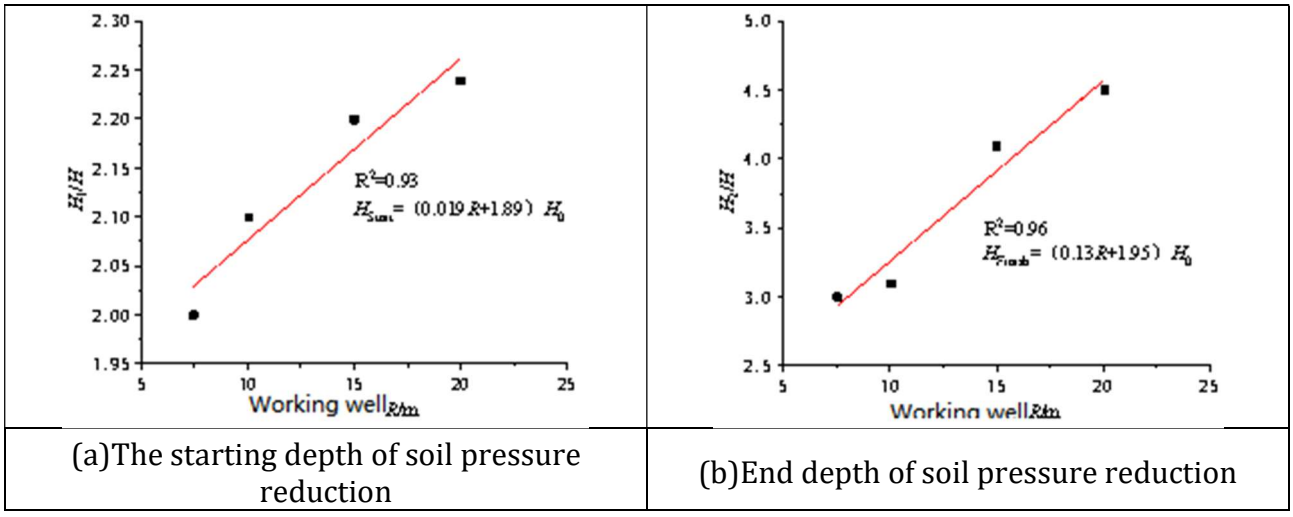

(a)The starting depth of soil pressure reduction

(b)End depth of soil pressure reduction

Figure 12. The relationship between the starting and ending depth and radius of the reduction of soil pressure in circular working wells

6.2. Example Demonstration of Circular Working Well

The actual size of the circular working well 4 # in the municipal comprehensive renovation project of Shanghai Hongqiao Business District is calculated by combining the above fitting formula to obtain the starting and ending depths of soil pressure reduction, as shown in Table 5. According to Figure 15, the maximum lateral displacement value of the retaining structure calculated by the plane elastic foundation beam method using the modified soil pressure distribution mode is 2.0mm, which is close to the measured value of 1.7mm, the 1.8mm obtained by the three-dimensional finite element method, and the 2.1mm obtained by the plane elastic foundation beam method using the standard soil pressure distribution mode. However, the plane elastic foundation beam method using a modified soil pressure distribution mode is simpler to model, more mature in parameter selection, and has lower computational costs compared to the three-dimensional finite element method. Compared with the plane elastic foundation beam method using a standardized soil pressure distribution mode, it is closer to the actual displacement direction.

ISSN: 2710-0588

Table 5. Depth of starting and ending points for soil pressure reduction

Excavation depth H_0(m)	The starting depth of soil pressure reduction H_{Start}(m)	End depth of soil pressure reduction H_{Finish}(m)
5	10.1	14.3
10	20.2	23(Under the wall)
15	23(Under the wall)	23(Under the wall)

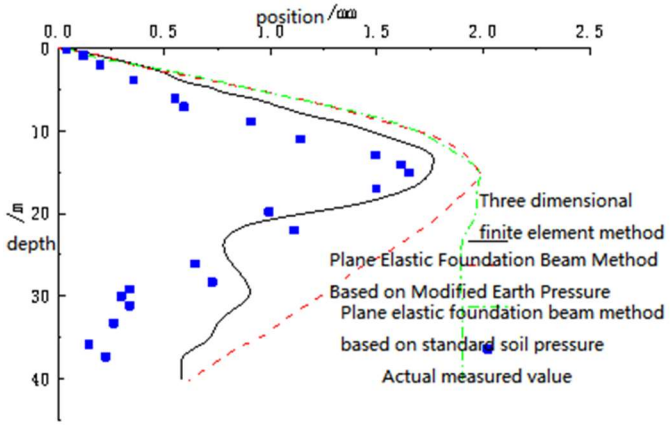

Figure 13. Comparison between calculated and measured lateral displacement values of circular working well enclosure structure

7. Conclusion

This article is based on the municipal comprehensive renovation project of Shanghai Hongqiao Business District, and conducts a study on the distribution pattern of soil pressure in circular working wells in soft soil areas. Based on the large-scale universal finite element software Abaqus, a three-dimensional numerical analysis model of well soil was established, taking into account factors such as wall insertion ratio, working well radius, wall thickness, and wall elastic modulus. The influence of working well spatial arch effect on the distribution mode of soil pressure was explored. On the basis of existing specifications [15], a distribution model of soil pressure in circular working wells in soft soil areas is proposed, and verified with engineering examples. The main conclusions are as follows:

(1) Based on the measured values, the three-dimensional numerical analysis model used in this article can better reflect the trend, maximum value, and corresponding position of the lateral displacement of the circular working well enclosure structure. However, the distribution pattern of soil pressure in existing specifications cannot reflect the true deep soil pressure, and there is a certain deviation between the calculated results and the actual situation.

(2) By exploring the influence of different influencing factors on the distribution pattern of soil pressure, it was found that the radius of the working well has a significant impact, while the wall insertion ratio, wall thickness, and wall elastic modulus have little effect.

(3) By modifying the existing specifications, a distribution model of soil pressure in circular working wells in soft soil areas was proposed, and a fitting formula for the reduction of soil pressure in circular working wells was obtained, which relates to the depth and radius of the starting and ending points.

(4) Through comparison, it was found that the modified earth pressure plane foundation beam method considering the circular arch effect is simpler, more mature in parameter selection, and has lower computational costs compared to the three-dimensional finite element method. Compared with the plane elastic foundation beam method that regulates earth pressure, it is closer to the actual displacement direction.

ISSN: 2710-0588

Acknowledgments

Natural Science Foundation.

References

[1] Yeqing Tang ,Qimin Li , Jiangyu Cui Analysis and Handling of Excavation Engineering Accidents [M] China Construction Industry Press, 1999.

[2] Xinping Dong , Qingha Guoi, Shunhua Zhou Analysis of deformation characteristics and main influencing factors of circular foundation pits [J] Journal of Underground Space and Engineering, 2005, 1 (2): 196-199.

[3] Minjian Long Reverse construction technology for lining of large-diameter vertical shaft with top pipe [J] Construction Technology, 2023: 176-179.

[4] Berezantzev The axial symmetry problem of ultimate equilibrium for loose soil [M] Construction Engineering Society, 1956.

[5] Prater E G. An examination of some theories of earth pressure on shaft linings[J]. Canadian Geotechnical Journal, 1977, 14(1): 91-106.

[6] Cheng Y M, Ya-Yuan H U. Active earth pressure on circular shaft lining obtained by simplified slip line solution with general tangential stress coefficient[J]. Chinese Journal of Geotechnical Engineering, 2005, 27(1): 110-115.

[7] Faqian Liu Research on the distribution pattern of soil pressure in circular foundation pits [D] Shanghai Jiao Tong University, 2008.

[8] Guoxiong Mei , Jinmin Zai An approximate calculation method for soil pressure considering the influence of displacement [J] Geotechnical Mechanics, 2001, 22 (1): 83-85.

[9] Jinmin, Zai Mei Guoxiong Research on Earth Pressure Model Considering Displacement [J] Journal of Nanjing Institute of Architecture and Engineering: Natural Science Edition, 2001 (1): 9-20.

[10] Jianping Zhao , Guoxiong Mei ,Jinmin Zai Research on the calculation method of soil pressure considering deformation and time effects [J] Journal of Yancheng Institute of Technology (Natural Science Edition), 2003, 16 (4): 1079-1082.

[11] Guosheng Lu A calculation method for soil pressure considering displacement [J] Geotechnical Mechanics, 2004, 25 (4): 586-589.

[12] Yekai Chen , Riqing Xu ,Chao Ren , etc Analysis of spatial effects in excavation of foundation pits [J] Building Structure, 2001 (10): 42-44.

[13] Yekai, Chen Riqing, Xu Xiaojun Yang , etc Calculation method for soil pressure of flexible retaining walls in foundation pit engineering [J] Industrial Architecture, 2001, 31 (3): 1-4.

[14] Yekai Chen Experimental study and numerical analysis of soil pressure on retaining walls [D] Zhejiang University, 2001.

[15] DGTJ08-61-2010, Technical Specification for Excavation Engineering [S] Shanghai Survey and Design Industry Association, Shanghai.

[16] Roscoe K H, Schofield A N, Thurairajah A. Yielding of Clays in States Wetter than Critical[J]. Geotechnique, 2015, 13(3): 211-240.

[17] Roscoe K H. On the generalised stress-strain behaviour of wet clay[J]. Engineering Plasticity, 1968:535-609.

[18] DGJ08-37-2012, Code for Investigation of Geotechnical Engineering [S] Shanghai Geotechnical Engineering Survey and Design Research Institute Co., Ltd., Shanghai.

[19] JGJ94-2008, Technical Specification for Building Pile Foundations [S] Ministry of Housing and Urban Rural Development of the People's Republic of China, Beijing.

[20] Shaoming Huang , Dazhao Gao Soft Soil Foundation and Underground Engineering -2nd Edition [M] China Construction Industry Press, 2005.

ISSN: 2710-0588

[21] Gao D Z, Wei D D, Hu Z X. Geotechnical Properties of Shanghai Soils and Engineering Applications[J]. ASTM, STP923, 1986, pp: 161-178.

[22] Daoduo Wei , Zhongxiong Hu Experimental study on the pre consolidation pressure and related compressibility parameters of shallow foundation soil in Shanghai [J] Journal of Geotechnical Engineering, 1980, 2 (4) 13-22.

[23] Xihong Zhao , Hongwei Jiang , Juyun, Yuan etc Shanghai Soft Soil Anisotropic Elastoplastic Model [J] Geotechnical Mechanics, 2003, 24 (3): 322-330.

[24] Zhonghua Xu Research on the deformation characteristics of deep foundation pits combined with support structures and main underground structures in Shanghai area [D] Shanghai Jiao Tong University, 2007.